

Understanding the Hydrogen/Ammonia Combustion Behaviours under Air and Oxygen Environments in a Combustion Chamber

Xiyao SUN¹, Chuan WANG², Yukun HU^{1*}

1 Department of Civil, Environmental & Geomatic Engineering, University College London, London, WC1E 6BT, UK

2 Swerim AB, Box 812, Luleå, SE-97125, Sweden

ABSTRACT

This paper dedicates to investigate the feasible and sustainable combustion fuel design which can be used to mitigate the environmental challenges posed by using conventional combustion fuel such as natural gas (CH₄) and propane (C₃H₈) in the industrial metal reheating processes. Three possible solutions were evaluated by using CFD method in Ansys Fluent: oxy-H₂, air-H₂ and air-NH₃/H₂. It has been found that oxy-H₂ combustion can simultaneously satisfy the requirement of both flame temperature and NO_x reduction. However, the use of oxy-H₂ solution might lead to high costs and a large amount of waste heat. The air-H₂ solution possesses the advantage of low cost and sufficient heat, but the NO_x emission is higher than that of propane combustion due to higher flame temperature. For the air-NH₃/H₂ solution, feasible combination schemes taking into consideration flame temperature, combustion efficiency and NO_x emissions were determined and ready to be analysed in terms of scale formation.

Keywords: oxy-H₂ and air-H₂ combustion, air-NH₃/H₂ combustion, metal reheating, reheating furnace, sustainable industrial fuel design, CFD simulation.

1. INTRODUCTION

The transition to a low-carbon/net-zero metal heating process will require the transformation of existing reheating furnaces and the development of new ones. Major investment is required that will take many years to be delivered. However, the transition pathway remains uncertain and, for much of the reheating furnace, the related technology deployments are still under debate. The present study focuses on the techno-economic feasibility of net-zero emission solutions for

metal heating, including air-H₂ combustion, oxy-H₂ combustion, and H₂/NH₃ co-combustion. The objective of this study is to investigate the characteristic of the three combustion modes in terms of ignition and combustion efficiency, and their integration with reheating furnaces to provide flexible metal heating operations for flame temperature control. The combustion of hydrogen (H₂) in different environments (i.e. oxygen and air) and with adding different proportions of ammonia (NH₃) is simulated by using the computational fluid dynamics (CFD) method. The flame temperature of each combustion scheme is investigated to compare with the conventional combustion source. In addition, the combustion products are also analysed to evaluate the environmental friendliness and cost-effectiveness of using H₂ and NH₃. Apart from that, the proportions of water vapour and oxygen (O₂) in the products of each combustion scheme are collected for the purpose of scale formation prediction in future research.

2. METHODOLOGY

In order to assess the combustion simulation of the candidate fuel supply scheme, CFD simulations were conducted by using Ansys Fluent. The geometrical model of the combustion chamber was built based on the chamber furnace at Swerim AB, as shown in Fig.1. The trials of propane (C₃H₈) combustion conducted on the furnace was simulated in order to validate the model. In the trials, the fuel with a constant injection rate of 0.00151 kg/s burns in the air environment with an air injection rate of 0.0276 kg/s and a preheat temperature of 500°C. The combustion was confined in the same

* Corresponding author. E-mail address: yukun.hu@ucl.ac.uk (Y. Hu)

chamber furnace with a constant wall temperature of 1250°C.

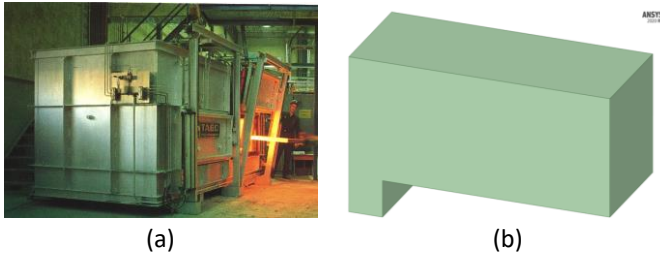


Fig. 1. Oil or propane fired chamber furnace at Swerim AB (a) and its geometry model (B)

The solving models applied in this simulation were mainly in accordance with the models adopted in Niska et al. [1] in order to form a comparison with the results obtained from the previous simulation. They include the finite rate/eddy dissipation two-step reaction model, discrete ordinates (DO) radiation model, and the standard κ - ω turbulence model. NO_x formation model was used to model the production of thermal and prompt NO_x for the case where applicable. Three different combustion solutions were investigated, including H₂ combusted in oxygen (oxy-H₂ solution), H₂ combusted in the air (air-H₂ solution), and H₂ and NH₃ co-combusted in the air (air-NH₃/H₂ solution). The oxy-H₂ and air-H₂ burner designs provided by Air Products Ltd. were used for modelling to adapt to different combustion environments. In the oxy-H₂ and air-H₂ combustion solutions, a fixed temperature of 1250 °C was specified to the chamber walls to simulate a temperature control mechanism on the chamber wall. In the air-NH₃/H₂ combustion solution, the adiabatic boundaries were adopted because the maximum combustion temperature of some fuel combination schemes might be lower than 1250°C, a fixed boundary temperature of 1250°C could obscure the simulation results and lead to a false comparison.

2.1 Oxy-hydrogen combustion (oxy-H₂) solution

In the modelling of the oxy-H₂ solution, the 3D hybrid hexahedral grid was adopted to mesh the chamber furnace with an oxy-fuel burner, as shown in Fig.2. Hexahedral mesh can fit in the burner design of the oxy-H₂ model perfectly. Compared to tetrahedral mesh, the hexahedral mesh is deemed to have higher accuracy. In order to balance the simulation accuracy and computation load, the combustion zone (i.e. the area that the flame is located, demonstrated as the darker colour area in Fig.2) was composed of finer cells, whereas the rest of the zones were filled with coarser cells. The total number of elements, in this case, is 509100,

connected by 530149 nodes, and the corresponding maximum mesh aspect ratio is 13.52. There are three hydrogen inlets and three oxygen inlets on the oxy-fuel burner installed in the front of the combustion chamber (Fig.2). The outlet of the chamber is located at the bottom of the combustion chamber near to the side of

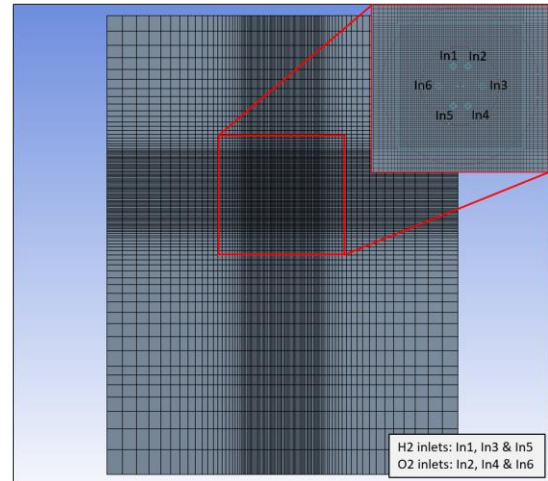


Fig. 2. Front view of the model mesh for the oxy-H₂ combustion solution

the burner. The operating conditions of the simulation cases of the oxy-H₂ solution are listed in Table 1. The stoichiometric ratio is given by Reaction 1.



Table 1. Operating conditions of the simulation cases of the oxy-H₂ solution

Burner capacity, kW	H ₂ supply rate, kg/s	O ₂ supply rate, kg/s
300	0.002	0.016
600	0.004	0.032
900	0.006	0.048

2.2 Air-hydrogen combustion (air-H₂) solution

In the modelling of the air-H₂ solution, the 3D hybrid tetrahedral grid was adopted to mesh the same chamber furnace with an air burner, as shown in Fig.3. In the generated tetrahedral grid, 212719 cells are mapped in total, and 44576 nodes are used to connect them. The air burner was installed at the same location as the oxy-fuel burner, as shown in Fig.3. Hydrogen fuel gas was designed to be injected into the chamber from a round shape inlet at the centre of the burner, and airflow comes into the chamber from the rectangular inlets which surround the hydrogen inlet.

Similar to the modelling of the oxy-H₂ solution, the reaction products and unreacted reactants are ejected from the bottom of the chamber. The operating conditions of the simulation cases of the air-H₂ solution

are listed in Table 2. The equivalent ratio of 1.03 was used in the simulation because the H₂ combustion efficiency in the air environment is less than that in the O₂ environment, an extra 3% of air is supplied to ensure complete combustion. The fuel and O₂ supply were calculated still based on Reaction 1, and the mass

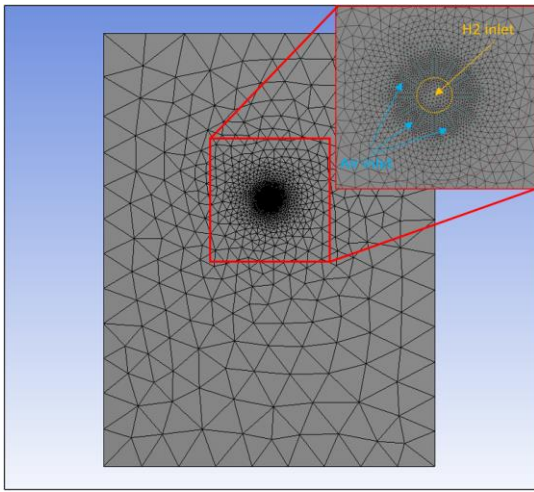


Fig.3. Front view of the model mesh for the oxy-H₂ combustion solution

fraction of O₂ in the air was set to 0.21.

Table 2. Operating conditions of the simulation cases of the air-H₂ solution

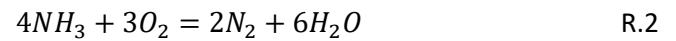
Burner capacity, kW	H ₂ supply rate, kg/s	Air supply rate, kg/s
300	0.002	0.071
600	0.004	0.141
900	0.006	0.212

2.3 - Air-ammonia and hydrogen co-combustion (Air-NH₃/H₂) solution

The modelling of air-NH₃/H₂ solution adopted the same chamber geometry and burner as the air-H₂ solution. Instead of the pure H₂ fuel gas, the mixture of H₂ and NH₃ fuel gas was injected into the chamber from the round shape inlet at the centre of the burner. The air-NH₃/H₂ are geometry was divided into 69859 cells connected by 13218 nodes. The mesh quality of the model was maintained within the acceptable range which the maximum aspect ratio should not be higher than 10.

In order to ensure the accuracy of the combustion of the H₂ and NH₃ mixture, a kinetic mechanism developed

by Otomo, et al. [2] was adopted in this simulation. This combustion kinetic mechanism was improved based on the mechanisms developed earlier by Klippenstein et al. [3] and Song et al. [4]. It consists of 32 species and 213 reactions. The improved mechanism has been proved that can more accurately predict flame speed, ignition delay, NH₃ concentration and NO_x generation in varying operation conditions such as pressure and stoichiometry ratio of NH₃/O₂ and NH₃/H₂/O₂ [2]. Eight different NH₃/H₂ ratios were designed with the equivalent ratio varying from a fuel-rich environment (0.7) to an air-rich environment (2.0); thus, 112 fuel combination schemes in total were designed in the present study. The detailed simulation schemes are listed in Table 3. The equivalent ratios were calculated based on Reaction 2, and the mass fraction of oxygen in the air was also set to 0.21.



3. RESULTS AND DISCUSSION

3.1 Model validation

Table 4 shows the results of propane combustion of the model in the reference report [1] and the model in the present study. It can be seen that the results obtained in the present study are in high accordance with the results reported in the reference document except for the residual O₂ and NO_x emission. Fig.4 demonstrates the temperature contours of C₃H₈ in the reference report [1], whereas the temperature contours of C₃H₈ obtained by using the present model is shown in Fig.5. It is evident that the flame temperature obtained by using the present model is in very good agreement with that of the reference case. However, the flame shape of the two cases seems to be different. The possible reason for the result difference, including O₂ residual and flame shape, could be that the different burner designs used in these two models. The burner with flame anchor used in the present study should possess higher combustion efficiency than the DFI burner used in the reference case [5]. However, similar to the result in the reference report, the NO_x level calculated is seen to be lower than the experimental result. This would indicate that modelling thermal and prompt NO_x is insufficient, and additional reactions are required. Nevertheless, taking into consideration that flame temperature and H₂O concentration of the

Table 3. The NH₃/H₂ ratios simulated in the air-NH₃/H₂ combustion solution

NH ₃ /H ₂ ratio								
Molar based	0.00/1.00	0.05/0.95	0.11/0.89	0.22/0.78	0.30/0.70	0.50/0.50	0.70/0.30	1.00/0.00
Mass based	0.00/1.00	0.30/0.70	0.50/0.50	0.70/0.30	0.78/0.22	0.89/0.11	0.95/0.05	1.00/0.00

Table 4. Comparison of the results of this research and the reference case

	Temp, °C	O ₂ , %	C ₃ H ₈ , %	H ₂ O, %	NO _x , mg/m ³
Reference	1720	2.57	-	13.20	135*
This study	1720	0.96	Traces	13.33	55

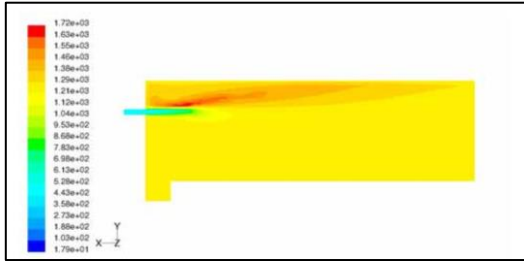


Fig.4. Temperature contours of air-C₃H₈ combustion in the reference case [1]

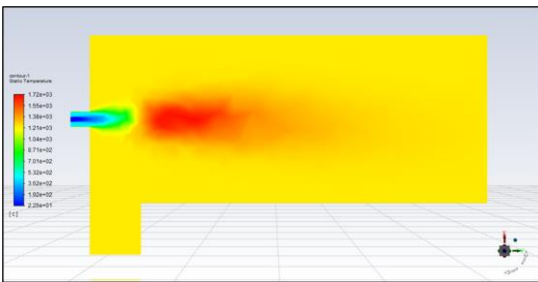


Fig.5. Temperature contours of air-C₃H₈ combustion simulated in this study

present study are in very good agreement with the reference case and the trend in NO_x generation, the model used in the present study can be deemed to have adequate accuracy and can be used in further simulations.

3.2 Oxy- and air-H₂ combustion solutions

Fig.6 shows a flame shape example of H₂ combustion in an O₂ environment in the present study. The simulation results of oxy-H₂ and air-H₂ combustion solutions are demonstrated in Fig.7, 8 and 9, respectively. It is evident that both flame temperature and volume average chamber temperature increase as the increase of H₂ supply for both simulations of the oxy-H₂ and air-H₂ combustion solutions (Fig.7). Compared to the reference case, the flame temperature produced by C₃H₈ combustion is slightly lower, which is only 1720 °C (Fig.4). As for the average chamber temperature, the values of air-H₂ solution (from 1775 °C to 1820 °C) are evidently higher than that of oxy-H₂ solution (1280 °C to 1341 °C). That is due to that the inflow velocity in the air-H₂ combustion is significantly higher than that in the oxy-H₂ combustion, and thus a higher momentum. The heat generated by combustion is more easily to be dispersed

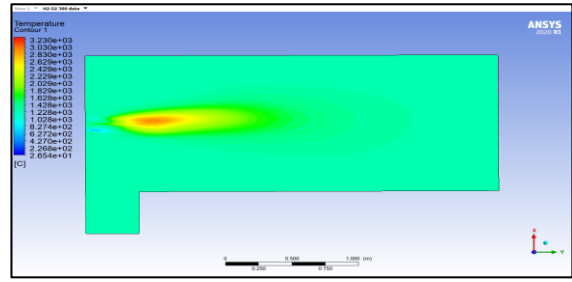


Fig.6. The temperature contours of oxy-H₂ combustion simulated in this study (300 kW, 0.002 kg/s H₂ and 0.016 kg/s O₂)

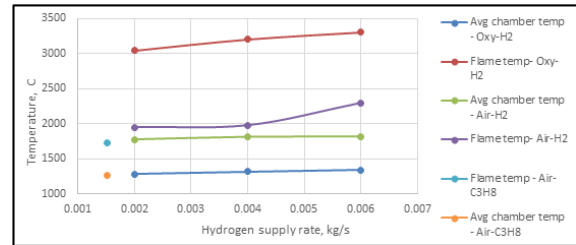


Fig.7. Flame temperature and volume average chamber temperature of the different combustion solutions simulated

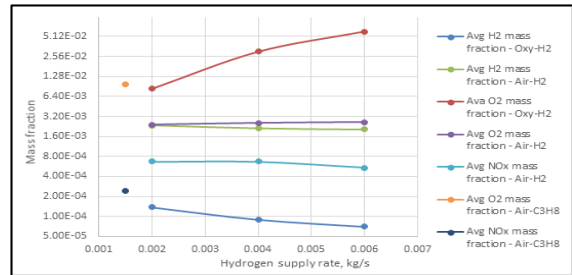


Fig.8. Average mass fractions of H₂, O₂ and NO_x of the different combustion solutions simulated

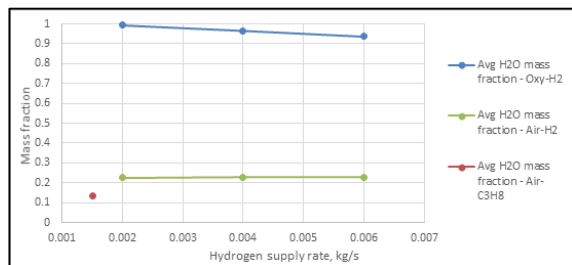


Fig.9. Average mass fractions of H₂O of the different combustion solutions simulated

within the chamber space through the convective heat transfer. This can also be reflected by the heat ratio between radiation source and reaction source. Simulation results indicate that the radiation/reaction heat ratio of oxy-H₂ solutions (0.79 for 300kW) are evidently higher than that of the air-C₃H₈ (0.58) solutions due to the lower convective heat transfer. The

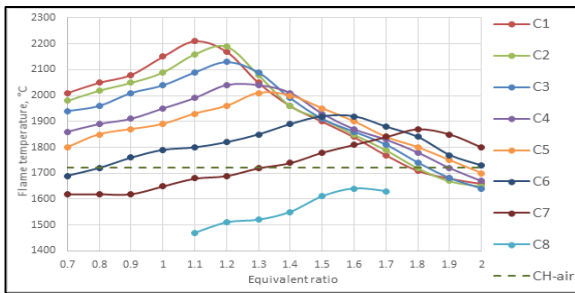


Fig.10. Flame temperature of air-NH3/H2 combustion under different NH3/H2 ratios and equivalent ratios

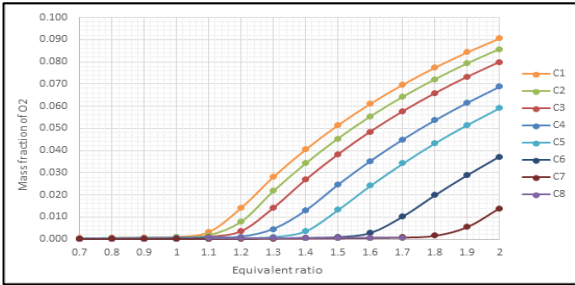


Fig.11. Residual O2 under different conditions of air-NH3/H2 combustion

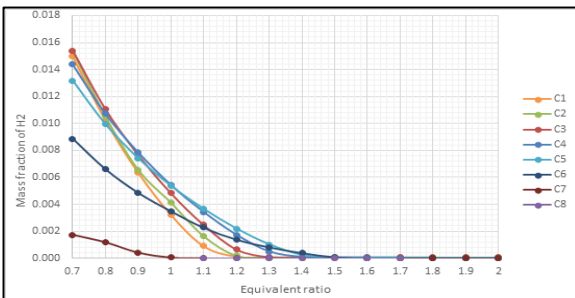


Fig.12. Unburn H2 under different conditions of air-NH3/H2 combustion

average chamber temperature of the reference case is the lowest among all the cases (1260°C); lower heating value and lower injection rate of C3H8 should be responsible for this result.

Fig.8 shows the simulated average mass fractions of H2, O2, and NOx for the air-C3H8, oxy-H2 and air-H2 combustion solutions, and Fig.9 shows the simulated average mass fraction of H2O for these combustion solutions. It will produce a more accurate comparison across different cases. The H2O and NOx produced in the reference air-C3H8 combustion are less than the air-H2

combustion solutions. Less H2O is due to the dilution by nitrogen contained in the air, and the lower NOx should be mainly as the result of the lower temperature. No NOx was produced due to lack of nitrogen in oxy-H2 solutions.

3.3 Air- NH3/H2 combustion solution

The combustion of the NH3/H2 mixture was investigated by manipulating the NH3/H2 ratio ρ and the equivalent ratio φ Fig.10 shows the dependence of adiabatic flame temperature in air-NH3/H2 combustion against the equivalent ratio φ and NH3/H2 ratio ρ . The obtained trends of results are in good agreement with the findings reported by Otomo, et al. [2], that is, the maximum adiabatic flame temperature rises with the increase of H2 mass fraction in supplied fuel.

Based on the experience of conventional hydrocarbon combustion, the ideal substitutes of conventional gas fuel should first satisfy the temperature requirement, that is, about 1700°C [1]. For comparison, the simulation cases of different combustion solutions with similar flame temperatures are listed in Table 5. It should be pointed out that, although there are combustion schemes that may result in the required flame temperature (the last two columns in Table 5), if it occurs to the left of the maximum flame temperature (Fig.10), it will result in incomplete combustion and thus low combustion efficiency. Furthermore, determination of the optimal fuel combination in practice should be carried on by taking into consideration other factors such as costs (e.g. fuel combustion efficiency and fuel usage) and scale formation.

Fig.11 shows the residual O2 in the furnace chamber, it can be seen that the residual O2 increases with the increase of equivalent ratio, and this trend becomes more evident as the H2 proportion in the fuel increases.

On the contrary, unburn H2 decreases as the equivalent ratio increases, as shown in Fig.12. Correspondingly, unburn NH3 also drop with the increase of air supply in a decreasing rate fashion (Fig.13). What is more, the results also show that the higher the NH3 proportion in the fuel, the higher the unburn NH3 will be found after the combustion due to the lower combustion efficiency determined by its chemical properties.

Table 5. Simulation cases that produce similar flame temperature to C3H8-air combustion

NH3/H2 ratio, molar based	0.00/1.00	0.05/0.95	0.11/0.89	0.22/0.78	0.30/0.70	0.50/0.50	0.50/0.50	0.70/0.30
Equivalent ratio	1.8	1.8	1.83	1.9	1.97	2.0	0.8	1.3
Flame temp, °C	1710	1720	1720	1720	1720	1730	1720	1720

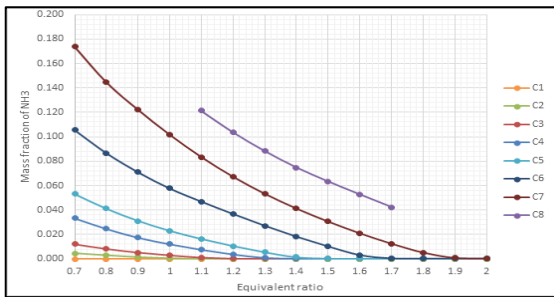


Fig.13. Unburn NH3 under different conditions of air-NH3/H2 combustion

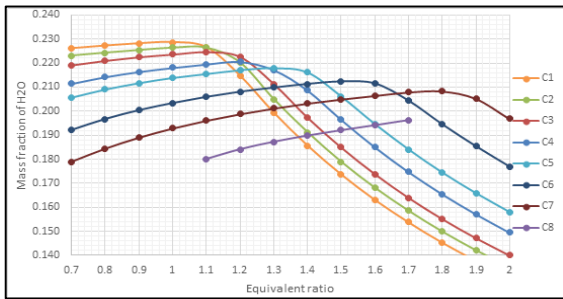


Fig.14. Produced H2O under different conditions of air-NH3/H2 combustion

Fig.14 shows the maximum amount of H₂O produced is higher when the H₂ proportion is higher, because H₂ combustion can produce more H₂O than the combustion of NH₃ with equal mass determined by their chemical reactions. The maximum H₂O mass fraction occurs approximately at the equivalent ratio which produces the maximum flame temperature. Residual O₂ and produced H₂O are two important criteria for the scale formation of steel slabs in the reheating process. Huitron et al. [6] pointed out an environment with high O₂ and H₂O proportion could facilitate the scale formation, together with the high temperature in reheating furnace, failure to control residual O₂ and produced H₂O could lead to a serious waste of fuel, raw materials and energy [7, 8].

4. CONCLUSIONS

This study mainly concerns the techno-economic feasibility and sustainability of alternatively combustion solutions which uses H₂ and the mixture of H₂ and NH₃ as the fuel to achieve the net-zero emission goal in metal reheating. By simulating the combustion behaviours of H₂ and NH₃/H₂ mixture in different environments, O₂ supply and combination ratios, it has been found that oxy-H₂ combustion exhibits the advantages of high combustion temperature and nearly zero NO_x emissions. However, it might result in a rise in costs due to pure O₂ supply. Apart from that, due to much less mass input but

higher heating value the flame temperature of the oxy-H₂ solution is evidently higher than the recommended temperature for steel reheating, but the average chamber temperature is less than that of the air-H₂ solution. Compared with the oxy-H₂ solution, the NO_x emissions are higher than that of the conventional combustion solution in the reference case because of the higher flame temperature. The simulation results of feasible NH₃/H₂ mixture schemes are obtained and analysed. The primary considerations are the satisfaction of flame temperature, combustion efficiency and sustainability. The obtained results can act as a guide for industrial fuel engineers to design the NH₃/H₂ mixture fuel based on the specific requirements of the equipment and projects.

ACKNOWLEDGEMENT

The authors would like to express their gratitude to the Engineering and Physical Sciences Research Council (EPSRC, EP/S018107/1), UK for the financial support for this work. Chuan Wang would like to acknowledge SK found (41.102403 .74 - FO REAG).

REFERENCES

- [1] Niska J, et al. Minimising NO_x emissions from reheating furnaces. 2007.
- [2] Otomo J, et al. Chemical kinetic modeling of ammonia oxidation with improved reaction mechanism for ammonia/air and ammonia/hydrogen/air combustion. *Int J Hydrogen Energy* 2018;43:3004–14.
- [3] Klippenstein SJ, et al. The role of NNH in NO formation and control. *Combust Flame* 2011;158:774–89.
- [4] Song Y, et al. Ammonia oxidation at high pressure and intermediate temperatures. *Fuel* 2016;181:358–65.
- [5] Klukas S, et al. Anchoring of turbulent premixed hydrogen/air flames at externally heated walls. *Int J Hydrogen Energy* 2020;45:32547–61.
- [6] Huitron RMP, et al. Scale formation on HSLA steel during continuous casting part ii: The effect of surface conditions. *Metals (Basel)* 2020;10:1–19.
- [7] Hu Y, et al. Modelling and simulation of steel reheating processes under oxy-fuel combustion conditions – Technical and environmental. *Energy* 2019:(under review).
- [8] Landfahner M, et al. Numerical and experimental investigation of scale formation on steel tubes in a real-size reheating furnace. *Int J Heat Mass Transf* 2019;129:460–7.